Fracture in Three-Dimensional Fuse Networks

G. George Batrouni[1,2] and Alex Hansen[3]
[1]*Institut Non-Linéaire de Nice, Université de Nice–Sophia Antipolis, 1361 route des Lucioles, F-06560 Valbonne, France*
[2]*Höchtleistungsrechenzentum, Forschungszentrum Jülich GMBH, D-52425 Jülich, Germany*
[3]*Institutt for Fysikk, Norges Teknisk-Naturvitenskapelige Universitet, NTNU, N-7034 Trondheim, Norway*
(Received 21 July 1997)

We report on large scale numerical simulations of fracture surfaces using random fuse networks for two very different disorders. There are some properties and exponents that are different for the two distributions, but others, notably the *roughness exponents*, seem universal. For the universal roughness exponent we found a value of $\zeta = 0.62 \pm 0.05$. In contrast to what is observed in two dimensions, this value is lower than that reported in experimental studies of brittle fractures, and rules out the minimal-energy surface exponent, 0.41 ± 0.01. [S0031-9007(97)05002-3]

PACS numbers: 62.20.Mk, 46.30.Nz

During the past ten years or so, fracture mechanics has caught the interest of the physics community. It is a field of utmost technological importance, and at the same time it poses fundamental questions on the interplay between disorder and dynamical effects. Early on, simple static models of brittle fracture, such as the *fuse model* [1], were constructed and studied extensively with the limited numerical tools of the time [2], which meant that only small two-dimensional systems were accessible. Even so, several qualitative and some quantitative results were obtained. Among the qualitative results, we may quote the existence of several types of fracture regimes depending on the type of initial disorder in the system [3,4]. The most notable quantitative result was the roughness of cracks obtained using the random fuse model [5]. This roughness, defined as a typical length scale associated with the direction perpendicular to the fracture plane, was found to scale with the linear size of the fracture plane to a power law with a roughness exponent $\zeta = 0.70 \pm 0.07$ for a wide class of different disorders. This exponent was later measured for two-dimensional stackings of collapsible cylinders [6] ($\zeta \approx 0.73$), for paper tear lines [7] ($\zeta = 0.68 \pm 0.05$), and for fractures in thin wood plates, where the grain structure was oriented parallel to the short axis ($\zeta = 0.68 \pm 0.04$) [8].

In three dimensions, studies of the scaling properties of fracture surfaces started with the work of Mandelbrot *et al.* [9]. Bouchaud *et al.* [10] suggested that the roughness exponent for brittle materials has a universal value close to 0.8. Later experimental work on a wide range of materials, e.g., by Måløy *et al.* [11], gave results which were consistent with such a hypothesis. However, Milman *et al.* [12] contested this hypothesis, and supported their claims with atomic force microscope measurements of fracture surfaces in crystalline metals. The picture that is emerging today is one where there is a smaller roughness exponent of about 0.4–0.5 at very small scales, which crosses over to a higher value ($\approx$0.8) at larger scales [13,14]. The smaller roughness exponent has been associated with slow crack propagation, where dynamical effects are negligible, while the higher crack speeds give rise to the higher value. It has been speculated that the smaller value is that of the minimum-energy surfaces [13], which by the best estimate of today is known to be 0.41 ± 0.01 [15]. We note that, in two dimensions, the corresponding minimal-energy surface problem leads to a roughness exponent equal to $2/3$, i.e., very close to that found in the fuse model.

Given the success of the fuse model in reproducing the experimentally observed roughness exponents in two dimensions, it is of great interest to test this model in three dimensions. As the fuse model does not contain any dynamical fracture properties, it is capable of isolating the effect of the interplay between the stress distribution (modeled as an electrical current distribution) and the distribution of local strengths in the material. It therefore models slow crack propagation. In particular, the hypothesis of a connection between the roughness exponent in this regime and that of the minimal-energy surfaces can be tested.

The model is a three-dimensional lattice with the nearneighbor sites connected by bonds, taken to be electrical fuses with identical resistance but whose burnout thresholds are disordered. A fuse conducts until the current it carries, i, exceeds the burnout (breaking) threshold, i_c, at which point it becomes irreversibly an insulator. The breaking thresholds, i_c, are drawn from some probability distribution (see below), and the potential difference across the $L \times L \times L$ lattice is applied along a diagonal of the cube, i.e., the $(1, 1, 1)$ direction. The finite-size effects associated with this choice are much smaller than taking the potential difference along a major lattice axis. To reduce finite-size effects further, we used periodic boundary conditions in *all* directions, i.e., we do not use actual planar electrodes attached to the lattice to apply the potential difference. Such electrodes greatly modify the behavior of the fracture surfaces in their neighborhood. Instead we use "ghost" sites that are not actually on the lattice to produce the potential difference [16].

So, a potential difference is applied and the weakest fuse is broken. To recalculate the currents in the bonds after a fuse has blown, one solves the Kirchhoff equations

by using the conjugate gradient algorithm, which is trivial, to parallelize efficiently. We did our simulations on the Connection Machine CM5. The stopping condition was that the residual error be less than 10^{-11}.

The system sizes we studied went from 8^3 to 48^3. The number of realizations per lattice depended on its size, on the type of disorder used, and the quantity studied. We list these numbers later on in the text.

The breaking thresholds were assigned by generating random numbers uniformly distributed on the unit interval and raising it to a power D. This corresponds to a cumulative probability distribution $P(i_c) = i_c^{1/|D|}$ when $D > 0$, and $P(i_c) = 1 - i_c^{-1/|D|}$ when $D < 0$. The smaller the value of $|D|$, the smaller the disorder. Furthermore, when $D > 0$ the distribution of strengths has a power law tail extending towards weak bonds (i.e., those with a small threshold), while when $D < 0$ the tail extends towards strong bonds. Depending on the value of D, the two-dimensional fuse model was shown to exhibit distinct classes of fracture behavior [4]. For small values of $|D|$, a macroscopic crack starts developing early in the fracture process, while when $|D|$ is large, a cloud of disconnected "microcracks" (blown fuses) develops before they coalesce into a final macroscopic crack. In the current paper, we study the fracture surfaces in three-dimensional systems with weak disorder, $|D| = 0.5$, i.e., macroscopic fracture surfaces start to develop early in the fracture process (localized fracture). To study universality issues we examined both positive and negative values of D, $D = \pm 0.5$. The idea is that, with such widely different distributions, universal and nonuniversal properties will be clearly distinguished.

Before turning to the question of fracture roughness, we report on some further results concerning the fracture process. These results should be compared with those obtained earlier for the two-dimensional fuse model [17,18], and for a three-dimensional elastic bond-bending model [19,20]. We find for $D = 0.5$ that $N_b \propto L^{2.6}$, while for $D = -0.5$ we find $N_b \propto L^{2.1}$, where N_b is the total number of broken bonds. The exponent 2.1 is consistent with 2, the trivial geometrical exponent of a surface, indicating that most of the broken bonds for this case belong to the fracture surface. The lack of universality for this exponent can be understood by examining the details of the formation of the fracture surface. Even though, for both positive and negative D, the simulations are done in the localized phases, the fracture surfaces evolve differently for each case. For the $D > 0$, the distribution allows for quite a few very weak bonds which must be broken before the fracture surface starts to develop. This initial breaking process is disorder dominated, and crosses over to current dominated breaking after enough bonds have been broken. At the crossover point, the fracture surface starts to develop and spread. But at this point there are already many broken bonds which do not belong to the fracture surface and which are randomly distributed in the *volume* of the lattice. On the other hand, we found that for $D < 0$ the breaking process starts out in the current dominated mode, for weak disorder, and so it is one of the very first broken bonds that determine where the fracture surface will start spreading. There are no broken bonds randomly distributed in the volume, in marked contrast with the $D > 0$ case. This result and its explanation are in agreement with those of [18] in two dimensions.

This same effect is clearly seen if one examines the evolution of the conductivity of the networks as a function of broken bonds. Figure 1 shows (for $L = 8$, 12, 16, 32, 48, $D = -0.5$) the conductivity as a function of "time," $t \equiv i/L^{\omega}$, where i is the number of broken bonds. We see that the data collapse is very good for $\omega = 2.13$ throughout the fracture process (except at the very end, where the finite-size effects are appreciable). On the other hand, positive D gives a very different picture. Figure 2 (inset) shows the conductivity versus $t = i/L^3$ for the same sizes as the previous case, but for $D = 0.5$. We see that, for times up to $t \approx 0.25$, the data collapse is excellent. In addition, we see that the scaling exponent 3 simply corresponds to the geometric dimension. As mentioned before, this is due to the fact that, for this case, the early times are disorder driven and therefore the broken fuses are randomly distributed in the volume, thus giving this geometric exponent. However, we also see that there is a sudden crossover to a different behavior. This is the crossover to the current driven regime. Figure 2, furthermore, shows the development of the conductivity but with the $t = i/L^2$ and where the curves are shifted to the right to coincide with the current driven curve for $L = 48$. We see that the data collapse in the current driven regime is excellent. This shows that in the *current driven* regime the fracture surfaces evolve at the same rate for all sizes and for both values of D (the two exponents, 2 and 2.13, are consistent). For $D > 0$ we find, in addition, that

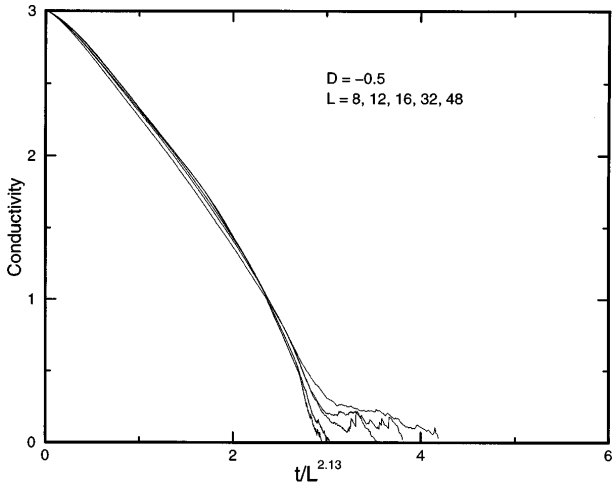

FIG. 1. Conductivity versus $t = i/L^{2.13}$ for $L = 8$ (200 realizations), 12 (200 realizations), 16 (200 realizations), 32 (64 realizations), and 48 (21 realizations). Here $D = -0.5$.

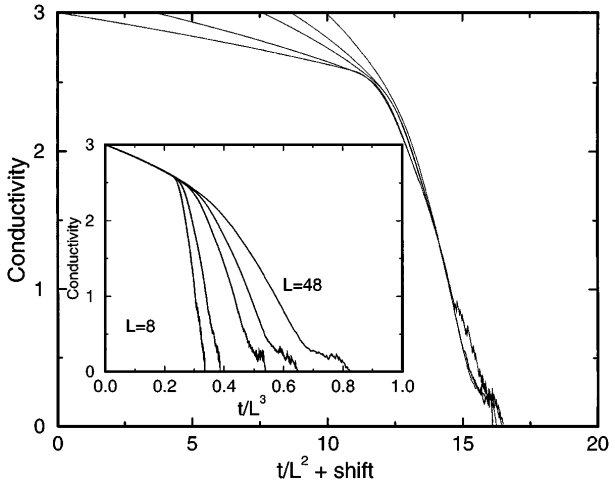

FIG. 2. Conductivity versus $t = i/L^2$ plus a shift making all curves collapse onto the $L = 48$ data late in the fracture process. The inset shows the conductivity as a function of $t = i/L^3$. The figures are based on $L = 8$ (200 realizations), 12 (200 realizations), 16 (144 realizations), 32 (62 realizations), and 48 (20 realizations). Here $D = 0.5$.

the number of bonds to be broken in order to cross over to the current dominated regime scales the same as $L^{2.7}$. The value found in [18] is 1.65 ± 0.03 for the two-dimensional case. This is consistent with our result in one additional dimension.

Figure 3 shows the I-V curves for $D = \pm 0.5$ and $L = 8$, 12, 16, 32, and 48. It shows clearly that the data follow the scaling law [17] $I = L^{\alpha} f(VL^{-\beta})$, where we found the best data collapse for $\alpha = 2$ and $\beta = 1$. These values are close to those found in [18] for two-dimensional systems, except that one must add 1 to α. This, of course, is not surprising since in three dimensions the current passes through a surface rather than a line as in two dimensions.

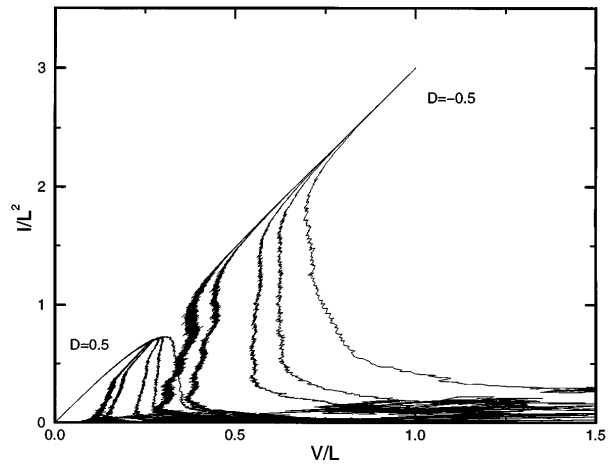

FIG. 3. The I-V characteristic for $D = 0.5$ and $D = -0.5$. The vertical axis shows I/L^2 as a function of V/L for $L = 8$, 12, 16, 32, and 48. Excellent data collapse is seen for the increasing part of the data. The number of configurations is the same as Figs. 1 and 2.

The universality of these exponents is very clear since the collapse is excellent for both $D = 0.5$ and $D = -0.5$. In addition, Fig. 3 shows that the two I-V characteristics are complimentary in the sense that the slopes of the scaling parts are identical.

Finally, we get to the roughness of the fracture surfaces. Our three-dimensional lattice has the topology of an S^3 torus. We cut it open in such a way that the fracture surface forms a square sheet, and we orient the surface in such a way that the z axis points along the $(1, 1, 1)$ direction, i.e., the mean current direction before any fuse has burned out. We measure the typical length scale W in the z direction using three different norms: (*i*) $\|\Delta z\|_2 = \sqrt{(\sum_i z_i^2)/N_s - (\sum_i z_i/N_s)^2}$, where z_i is the z coordinate of the ith broken bond belonging to the fracture surface and N_s is the total number of these; (*ii*) $\|\Delta z\|_\infty = (\max_i z_i - \min_i z_i)$; and (*iii*) the smallest eigenvalue of the moment of inertia tensor of the fracture surface, $I_{\min}$. Figure 4 shows W as a function of L based on these three norms for the two types of disorder. For $D = 0.5$, lattice sizes are $L = 8$, 12, 16, 32, 48 with 600, 200, 402, 146, 133, 37 realizations, respectively, and for $D = -0.5$, the sizes are $L = 8$, 12, 16, 32, 48 with 300, 200, 200, 64, 21 realizations, respectively. The figure shows that there is no appreciable difference in roughness between the two types of disorder used. There are strong finite-size corrections to the power laws that the different kinds of roughness measures follow. However, the way these corrections affect the asymptotic power laws depends on the measures. For the $\|\Delta z\|_\infty$, the effective roughness exponent approaches the asymptotic one from above, while for the $\|\Delta z\|_2$ and $I_{\min}$ measures, the asymptotic roughness exponent is approached from below. In Fig. 5, we show the effective roughness exponents, defined as $[\ln W(L') - \ln W(L)]/[\ln L' - \ln L]$, based on these measures for both the $D = 0.5$ and $D = -0.5$

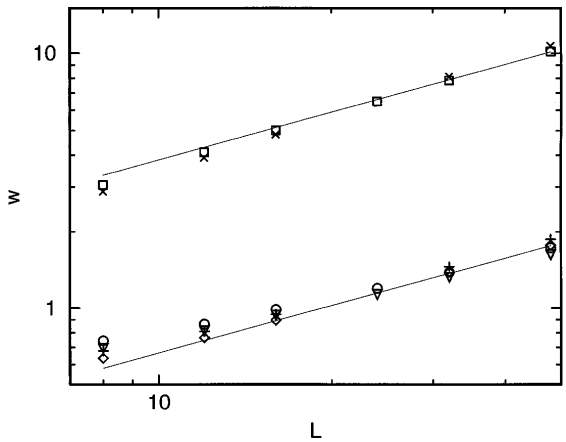

FIG. 4. Roughness W as a function of linear lattice size L, where W has been estimated from (*i*) $\|\Delta z\|_2$, $D = 0.5$ (circles) and $D = -0.5$ (plus); (*ii*) $\|\Delta z\|_\infty$, $D = 0.5$ (crosses) and $D = -0.5$ (squares); and (*iii*) $I_{\min}$, $D = 0.5$ (triangles) and $D = -0.5$ (diamonds). The slope of the two straight lines is 0.62.

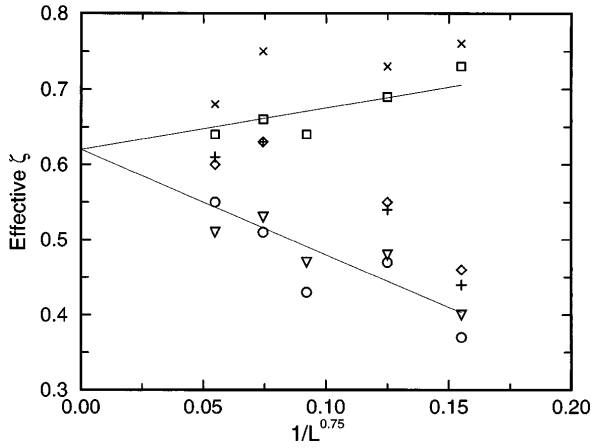

FIG. 5. Effective roughness exponent, ζ_{eff} as a function of L based on (*i*) $\|\Delta z\|_2$, $D = 0.5$ (circles) and $D = -0.5$ (plus); (*ii*) $\|\Delta z\|_\infty$, $D = 0.5$ (squares) and $D = -0.5$ (crosses); and (*iii*) I_{min}, $D = 0.5$ (triangles) and $D = -0.5$ (diamonds). The two straight lines are guides to the eye.

disorders, plotted against $L'^{-0.75}$. Two straight lines have been added, which somewhat follow the $\|\Delta z\|_\infty$, $D = 0.5$ data and the $\|\Delta z\|_2$, $D = 0.5$ data. They act as guides to the eye. Based on this figure, we suggest an asymptotic roughness exponent equal to $\zeta = 0.62 \pm 0.05$ for both disorders.

We see that this value is smaller than the value of 0.8 typically seen in large scale brittle fractures. It is, however, also larger than the value seen at small scales, which is of the order 0.4–0.5. Our result, $\zeta = 0.62 \pm 0.05$, seems to rule out the minimal-energy exponent, 0.41 ± 0.01, advocated for slowly propagating cracks. Thus, the coincidence between the roughness exponent found in the two-dimensional fuse model and the corresponding minimal-energy problem seems fortuitous.

We thank S. Roux for many valuable discussions. We also thank Thinking Machines Corp. for (almost unlimited) computer time on their CM5s. Travel support was provided by the CNRS and the NFR through a PICS grant.

[1] L. de Arcangelis and H. J. Herrmann, J. Phys. Lett. (France) **46**, L585 (1985).
[2] *Statistical Models for the Fracture of Disordered Materials*, edited by H. J. Herrmann and S. Roux (Elsevier, Amsterdam, 1990).
[3] B. Kahng, G. G. Batrouni, S. Redner, L. de Arcangelis, and H. J. Hermann, Phys. Rev. B **37**, 7625 (1988).
[4] A. Hansen, E. L. Hinrichsen, and S. Roux, Phys. Rev. B **43**, 665 (1991).
[5] A. Hansen, E. L. Hinrichsen, and S. Roux, Phys. Rev. Lett. **66**, 2476 (1991).
[6] C. Poirier, M. Ammi, D. Bideau, and J. P. Troadec, Phys. Rev. Lett. **68**, 216 (1992).
[7] J. Kertesz, V. K. Horvath, and F. Weber, Fractals **1**, 67 (1993).
[8] T. Engøy, K. J. Måløy, A. Hansen, and S. Roux, Phys. Rev. Lett. **73**, 834 (1994).
[9] B. B. Mandelbrot, D. E. Passoja, and A. J. Paullay, Nature (London) **308**, 721 (1984).
[10] E. Bouchaud, G. Lapasset, and J. Planès, Europhys. Lett. **13**, 73 (1990).
[11] K. J. Måløy, A. Hansen, and S. Roux, Phys. Rev. Lett. **68**, 213 (1992).
[12] V. Yu. Milman, R. Blumenfeld, N. A. Stelmashenko, and R. C. Ball, Phys. Rev. Lett. **71**, 204 (1993).
[13] E. Bouchaud and J. P. Bouchaud, Phys. Rev. B **50**, 17 752 (1994).
[14] E. Bouchaud and S. Navéos, J. Phys. I (France) **5**, 547 (1995).
[15] A. A. Middleton, Phys. Rev. E **52**, R3337 (1995).
[16] S. Roux (unpublished).
[17] L. de Arcangelis, A. Hansen, H. J. Herrmann, and S. Roux, Phys. Rev. B **40**, 877 (1989).
[18] L. de Arcangelis and H. J. Herrmann, Phys. Rev. B **39**, 2678 (1989).
[19] S. Arbabi and M. Sahimi, Phys. Rev. B **41**, 772 (1990).
[20] M. Sahimi and S. Arbabi, Phys. Rev. B **47**, 713 (1993).